Life Sciences 232 (2019) 116628

Contents lists available at ScienceDirect

Life Sciences

journal homepage: www.elsevier.com/locate/lifescie

Thymoquinone enhances the anticancer activity of doxorubicin against adult T-cell leukemia *in vitro* and *in vivo* through ROS-dependent mechanisms

Maamoun Fatfat[a,b], Isabelle Fakhoury[a,1], Zeina Habli[a,1], Rasha Mismar[a], Hala Gali-Muhtasib[a,b,*]

[a] Department of Biology, Department of Anatomy, Cell Biology and Physiological Sciences, American University of Beirut, Riad El Solh, 1107 2020, Beirut, Lebanon
[b] Center for Drug Discovery, American University of Beirut, Lebanon

ARTICLE INFO

Keywords:
Apoptosis
Combination therapy
Doxorubicin
Leukemia/lymphoma
Thymoquinone

ABSTRACT

Aims: Adult T-cell leukemia (ATL) is a mature T-cell neoplasm associated with human T-cell lymphotropic virus (HTLV-1) infection. Major limitations in Doxorubicin (Dox) chemotherapy are tumor resistance and severe drug complications. Here, we combined Thymoquinone (TQ) with low concentrations of Dox and determined anticancer effects against ATL in cell culture and animal model.

Main methods: HTLV-1 positive (HuT-102) and HTLV-1 negative (Jurkat) CD4+ malignant T-cell lines were treated with TQ, Dox and combinations. Viability and cell cycle effects were determined by MTT assay and flow cytometry analysis, respectively. Combination effects on mitochondrial membrane potential and generation of reactive oxygen species (ROS) were assessed. Expression levels of key cell death proteins were investigated by western blotting. A mouse xenograft model of ATL in NOD/SCID was used for testing drug effects and tumor tissues were stained for Ki67 and TUNEL.

Key findings: TQ and Dox caused greater inhibition of cell viability and increased sub-G1 cells in both cell lines compared to Dox or TQ alone. The combination induced apoptosis by increasing ROS and causing disruption of mitochondrial membrane potential. Pretreatment with N-acetyl cysteine (NAC) or pan caspase inhibitor significantly inhibited the apoptotic response suggesting that cell death is ROS- and caspase-dependent. TQ and Dox combination reduced tumor volume in NOD/SCID mice more significantly than single treatments through enhanced apoptosis without affecting the survival of mice.

Significance: Our combination model offers the possibility to use up to twofold lower doses of Dox against ATL while exhibiting the same cancer inhibitory effects.

1. Introduction

Adult T-cell leukemia (ATL) is an aggressive malignancy linked to the transformation of CD4+ helper T-cells by human T-cell lymphotropic virus 1 (HTLV-1) [1]. Only 3–5% of patients develop ATL post infection after a long latent period [2]. HTLV-1 is a retrovirus with single stranded RNA coding for oncogenic proteins [3]. Tax, a pleiotropic viral protein, is a transcriptional transactivator essential for immortalization of T-cells [4,5] through creating genetic instabilities, amplifying centrosomes, inducing clastogenic DNA damages, abrogating p53 tumor-suppressor protein, and constitutively activating the nuclear factor κB (NFκB) signaling pathway [6,7]. Cumulatively, these modulations repress infected cells to undergo apoptosis. Over the last 2 decades, immense therapeutic approaches have been tested against ATL but more efforts are needed to find selective anticancer drugs with less adverse side effects.

Thymoquinone (TQ), the active ingredient of *Nigella sativa* black seed, exhibits promising therapeutic potential against a wide range of biological conditions particularly cancer [8–10]. TQ was shown to be effective in inhibiting the growth and proliferation of many chemoresistant cancer cell lines, arresting cancer cells at different phases of the cell cycle, and interrupting their invasion and metastasis [9]. Recent attempts in our laboratory showed that TQ induces a time- and dose-dependent caspase activated apoptosis against both HTLV-1 positive and HTLV-1 negative CD4+ malignant T-cells [11]. Our findings revealed that TQ enhanced the generation of reactive oxygen species (ROS) and downregulated glutathione (GSH) levels [11].

Doxorubicin (Dox), an antibiotic isolated from *Streptomyces*

* Corresponding author at: Department of Biology, American University of Beirut, Riad El Solh, 1107 2020, Beirut, Lebanon.
E-mail address: amro@aub.edu.lb (H. Gali-Muhtasib).
[1] Equally contributed.

https://doi.org/10.1016/j.lfs.2019.116628
Received 28 January 2019; Received in revised form 23 June 2019; Accepted 1 July 2019
Available online 03 July 2019
0024-3205/

peucetius, is used in clinic to treat solid and hematological tumors including acute leukemia, but reports of early onset of tumor resistance is a major limitation in Dox chemotherapy [12]. Combination therapies are the new trend in cancer treatment, particularly due to tumor resistance and drug-induced severe side effects [13]. Evidence indicates that combining TQ with clinical drugs enhances their therapeutic index and/or lessens their cytotoxicity against non-tumor tissues [10,14]. Studies have also shown that TQ improves the anticancer potential of Dox in HL-60 myeloblastic leukemia and multi-drug-resistant MCF-7/TOPO breast cancer cells by ROS production and mitochondria associated apoptosis [15]. In another study, TQ enhanced apoptosis in Dox-resistant human breast cancer cells MCF-7/Dox by PTEN up-regulation and Akt phosphorylation inhibition [16]. At least three animal studies have presented evidence for a protective role of TQ against Dox-induced cytotoxicity, mainly against nephrotoxicity and cardiotoxicity [17–19]. In light of the promising potential of TQ in combination studies, we sought to combine Dox with TQ and investigate their anticancer potential against ATL *in vitro* and *in vivo*. The cytotoxicity and anticancer potential of single treatments or TQ and Dox combinations was investigated in HTLV-1 positive HuT-102 and HTLV-1 negative Jurkat cells. We also investigated drug-induced mechanisms of cell death and effects on ROS generation, mitochondrial membrane potential and the expression of target proteins involved in cell cycle modulation and cell death. Finally, we developed an ATL xenograft model and assessed the *in vivo* anticancer potential of TQ and Dox on tumor volume and on markers of proliferation and apoptosis.

2. Materials and methods

2.1. Materials

RPMI 1640 with 25 mm HEPES and L-glutamine, fetal bovine serum (FBS), trypsin, penicillin-streptomycin (P/S), N-acetyl cysteine (NAC), *Z*-VAD-fmk, Dulbecco's phosphate buffered saline (PBS), bovine serum albumin (BSA), and trypan blue were purchased from Sigma (St. Louis, Missouri, USA). Propidium iodide (PI), and 1,2 dimethylsulfoxide (DMSO) were obtained from Molecular Probes (Eugene, Oregon, USA). RNAse A and protease inhibitor were ordered from Roche (Mannheim, Germany). Rhodamine 123 and CM-H2DFCDA were purchased from Invitrogen. PVDF membranes were obtained from Amersham Pharmacia Biotech (Amersham, England).

2.2. Cell culture and treatment

Human HTLV-1 positive (HuT-102) and HTLV-1 negative (Jurkat) CD4+ malignant T-cell lines were cultured in RPMI 1640 medium (Invitrogen Molecular Probes, Eugene, OR, USA) supplemented with 10% heat inactivated fetal bovine serum (FBS) and 1% penicillin streptomycin. Cells were grown in a humidified incubator (95% air, 5% CO_2) and media was replenished every two days. At 70% confluency, cells were passaged as follows: cells and media were aspirated from the flask, placed in a conical tube then centrifuged at 1200 rpm for 5 min. The supernatant was discarded and the cells were resuspended in fresh RPMI 1640 medium. Finally, the cells were either re-plated in T75 or T175 flasks for expansion of cells, seeded for experimentation, or frozen and stored at −196 °C in liquid nitrogen. TQ and Dox were dissolved in methanol and DMSO, respectively. TQ concentrations of 10 and 40 μM and Dox concentrations of 50 and 100 nM were prepared by serial dilutions in the cell culture media. The final DMSO concentration on cells to cells was < 0.1%. Unless otherwise mentioned, cells were seeded (2×10^5 cells/ml) and treated at 50% confluency with Thymoquinone (MP Biomedicals, France) and Doxorubicin with the desired concentration for 24 or 48 h. For most studies, Jurkat cells were treated with 10 μM TQ, 50 nM Dox or their combination for 24 h while 40 μM TQ, 100 nM and their combination were used for the treatment of HuT-102 cells for 48 h.

2.3. MTT assay

HuT-102 and Jurkat cells were seeded (1×10^5 cells/ml) in 96-well plates and treated with Dox at different concentrations for 24 or 48 h. Proliferation was assessed by the Cell Titer 96-non-radioactive cell proliferation assay kit according to manufacturer's instructions (Promega Corp, Madison, WI, USA). In this assay, the ability of metabolically active cells to convert 3-(4,5-dimethyl thiazol-2-yl)-2,5-diphenyl tetrazolium bromide (MTT) into a blue formazan product was measured and its absorbance was recorded at 595 nm using an enzyme linked immuno-sorbent assay (ELISA) microplate reader. Results are expressed as % of viable cells relative to control. The following formula was used to calculate the % of viable cells.

% viability = [mean O.D. treatment/mean O.D. control] × 100.

2.4. Trypan blue assay

Trypan blue dye exclusion assay was used to evaluate the efficacy of separate or combined TQ and Dox treatments in comparison to control untreated cells. Cells were seeded in 12-well plates at a density of 10^5 cells/ml. At 50% confluency, cells were treated in triplicate with the different TQ and Dox concentrations as well as their combinations. Then, cells were mixed with equal volumes of dye and mounted on a hemocytometer for counting under the microscope. Results are expressed as % of viable cells relative to control. The following formula was used to calculate the % of viable cells.

% viability = [number of viable cells (treatment)/number of viable cells (control)] × 100.

2.5. Cell cycle analysis

Jurkat and HuT-102 cells were seeded in 6-well plates at a density of 2×10^5/ml and incubated overnight. After treatment with the corresponding time points, the cells were collected and washed twice with 1× PBS, fixed in 70% ice-cold ethanol, and stored at −20 °C overnight. Subsequently, cells were washed twice with PBS, incubated for 30 min at 37 °C with 300 μl PBS, 125 μl RNase, and 25 μl PI (1 mg/ml). Supernatants were then transferred to flow tubes, the samples were excited at 535 nm and the fluorescence recorded at 635 nm. A FACS scan flow cytometer from Becton Dickinson was used to record 10,000 ungated events. Analysis of the events was performed using the Cell Quest software (Becton Dickinson).

2.6. TUNEL assay

For TUNEL assay, 2×10^5 cells were seeded in 6-well plates and incubated overnight before treatment. Fragmented DNA was quantified by the terminal deoxytransferase-mediated dUTP nick-end labeling assay (TUNEL). Jurkat and HuT-102 cells were collected post-treatment, washed twice with PBS, resuspended in 4% formaldehyde and incubated at room temperature for 30 min. Cells were then pelleted, washed with PBS, resuspended in 100 μl solution containing PBS, 0.1% sodium citrate, and 0.1% Triton X-100 and incubated for 2 min on ice. After a second wash step, the cells were incubated for 1 h in 50 μl TUNEL reaction mixture consisting of 45 μl of the labeling solution and 5 μl of the enzyme solution. After incubation in the dark in a humidified atmosphere (37 °C), the mixture was washed and the cells were suspended in 450 μl PBS for flow cytometry analysis. The cells were excited using the 494 nm wavelength and the results recorded at the 521 nm wavelength.

2.7. Mitochondrial membrane potential by rhodamine staining

The mitochondrial membrane potential was measured using rhodamine 123; a green fluorescent dye which accumulates in active mitochondria with high membrane potential. Jurkat and HuT-102 cells

were treated with TQ, Dox, and combinations with or without pre-treatment with 5 mM NAC (2 h) or with 10 μM of the general caspase inhibitor pan caspase. After treatment, the cells were collected and the pellets were washed twice in rhodamine buffer. The cells were then stained at 37 °C in the dark for 30 min using a rhodamine 123 dye solution (5 μM). Finally, the cells were washed and resuspended in rhodamine buffer before analysis by flow cytometry. The cells were excited at 488 nm and the emission recorded at 525 nm.

2.8. Measurement of ROS

Generation of intracellular H_2O_2 was measured using 5-(and-6)-chloromethyl 2′,7′-dichlorodihydrofluorescein diacetate acetyl ester (CM-H2DCFDA) kit. At 50% confluency, cells were collected and washed with PBS then resuspended in 500 μl RPMI medium containing 2% FBS and 10 μM CM-H2DCFDA. The incubation was performed at 37 °C, in the dark for 20 min. Subsequently, Jurkat and HuT-102 cells were treated for 1 h with TQ, Dox, the combination (with or without pre-treatment with 5 mM NAC for 2 h) or with H_2O_2 (150 μM). The medium was then removed and the cells were washed twice and resuspended in 500 μl of PBS prior to analysis with a FACS scan flow cytometer. The cells were excited using the 494 nm wavelength and the results recorded at the 521 nm wavelength.

2.9. Protein extraction and Western blotting

For Western blot analysis, cells were seeded in T75 flasks, treated with the corresponding concentrations and collected at different time intervals after treatment. The cell pellets were washed with 1× PBS then lysed in ice-cold radio immunoprecipitation buffer (RIPA (TNE) - 10 mM Tris-HCl-pH 7.8, 1% NP40, 0.15 M NaCl, 1 mM EDTA) after the addition of phosphatase II arrest, phosphatase III arrest and protease inhibitors. Protein concentration in the cell lysate was determined using Lowry Assay. BSA was used as a standard for protein quantification. On the basis of equal protein loading, 40 μg of protein extracts was separated by SDS-PAGE on a 12% and 15% denaturing polyacrylamide gel, transferred to a nitrocellulose membrane (Bio-Rad) and blocked with blocking buffer (*i.e.* TBS-Tween 20 containing 5% non-fat milk or BSA) for 1 h at room temperature. The membranes were then incubated overnight with the appropriate primary antibodies at 5 °C. The bound antibody was detected using peroxidase-conjugated anti-rabbit antibody (1:10000) or anti-mouse antibody (1:10,000) purchased from Santa Cruz Biotechnology Inc., California, USA followed by chemiluminescence (ECL System) and exposed to autoradiography.

2.10. Mouse xenografts

NOD/SCID mice (6–8 weeks, ~20 g) were divided into four groups (6 mice each) and maintained in Maxi-miser hepafiltered facility. 7.5×10^6 HuT-102 tumor cells in 100 μl Media:Matrigel (1:1 ratio) were inoculated subcutaneously in the right flank. Prior to manipulations, mice were anesthetized with isoflurane (Forane®, Abbott) by inhalation. TQ and Dox were dissolved in methanol first and then diluted in lipofundin® MCT/LCT 20% such that the final concentration of methanol did not exceed 0.1% to avoid toxicity to mice. On day 9 post cell inoculation, mice received intraperitoneal (i.p.) injections of either lipofundin® (control), 20 mg/kg of TQ (three times a week), 0.5 mg/kg of Dox (once a week) or TQ and Dox combinations for 23 days. Tumor measurements were performed 3 times per week using a sterile Vernier caliper. Tumor volume was calculated by the formula: Volume = π/6*(length × width × height). All mice appeared healthy and tolerated the drug treatment well. The use of laboratory animals was in accordance with the guidelines of the Institutional Animal Care and Use Committee (IACUC) at the American University of Beirut.

2.11. Immunohistochemistry of mouse tissues

At the end of the animal studies, all mice were euthanized by isoflurane overdose and tumor tissues were collected for further histological and immunohistochemical analysis. Tissue sections (4 μm) were stained with anti-Ki-67 antibody (Santa Cruz, USA) for 60 min followed by secondary and tertiary antibodies and incubated with chromogen (Zymed, USA) before counter staining with Hematoxylin. To assess the extent of total cell death, tissue sections were stained using the terminal deoxyribonucleotidyl transferase-mediated dUTP-nick-end labeling (TUNEL) assay according to manufacturer's instructions (*in situ* cell death detection kit fluorescein; Roche). Cells were counter-stained with DAPI and slides were analyzed under Leica Fluorescent microscope. Ki-67 and TUNEL staining was quantified by Image J. Tissue section images were inverted to black and white by the thresholding method and positively stained cells were analyzed and counted. The following formula was used to calculate the % of positive cells: % positive cells = [positively stained cells/total cells] × 100.

2.12. Statistical analysis

To determine the statistical significance between two samples, two-tailed student *t*-test was used (Microsoft Office Excel). One-way analysis of variance (ANOVA) was used to test for statistical significance between multiple samples. Statistically significant results compared to the untreated control were assigned as $*p < 0.05$ and $**p < 0.01$.

3. Results

3.1. TQ and Dox combination reduce the viability of Jurkat and HuT-102 cells to a greater extent than Dox alone

First, we tested the effect of Dox alone on HTLV-1 positive (HuT-102) and HTLV-1 negative (Jurkat) malignant CD4+ T-cells. HuT-102 and Jurkat cells were treated with Dox at concentrations ranging between 50 and 750 nM for 24 or 48 h after which cell viability was determined by MTT assay. The results in Fig. 1a show a time- and dose-dependent response to Dox treatment in both Jurkat and HuT-102 cells. The HTLV-1 negative cells were more sensitive than the HTLV-1 positive cells to Dox treatment at 48 h. The IC_{50} value for Jurkat was around 50 nM at 48 h as compared to 100 nM for the HuT-102 cells at the same time point.

Next, we tested whether the combination of Dox and TQ causes enhanced anticancer effects against Jurkat and HuT-102 cells. Briefly, several concentrations of Dox ranging between 50 and 100 nM were combined with several concentrations of TQ ranging between 5 and 40 μM and their effects on the viability of both cell lines were tested at 24 and 48 h post-treatment. As shown in Fig. 1b and c, TQ and Dox combinations reduced the viability of Jurkat and HuT-102 cells more effectively compared to each drug alone in a time-dependent manner. Trypan exclusion assay confirmed the MTT results. (Sup. Fig. 1).

For upcoming experiments, we investigated only two combination mixtures of TQ and Dox that significantly inhibited cell viability while circumventing the need to use high doses of Dox to achieve the same effect. These combinations included 10 μM of TQ with 50 nM Dox against Jurkat cells, and 40 μM of TQ with 100 nM Dox against HuT-102 cells. Both combinations caused 70 to 80% inhibition in cell viability at 48 h post-treatment in both Jurkat and HuT-102 cells (Fig. 1b and b).

3.2. TQ and Dox combination increases the sub-G1 population in Jurkat and HuT-102 cells

To determine whether the inhibition of viability by TQ and Dox combination was due to cell cycle arrest and/or apoptosis, cell cycle analysis was performed using propidium iodide (PI) staining of DNA

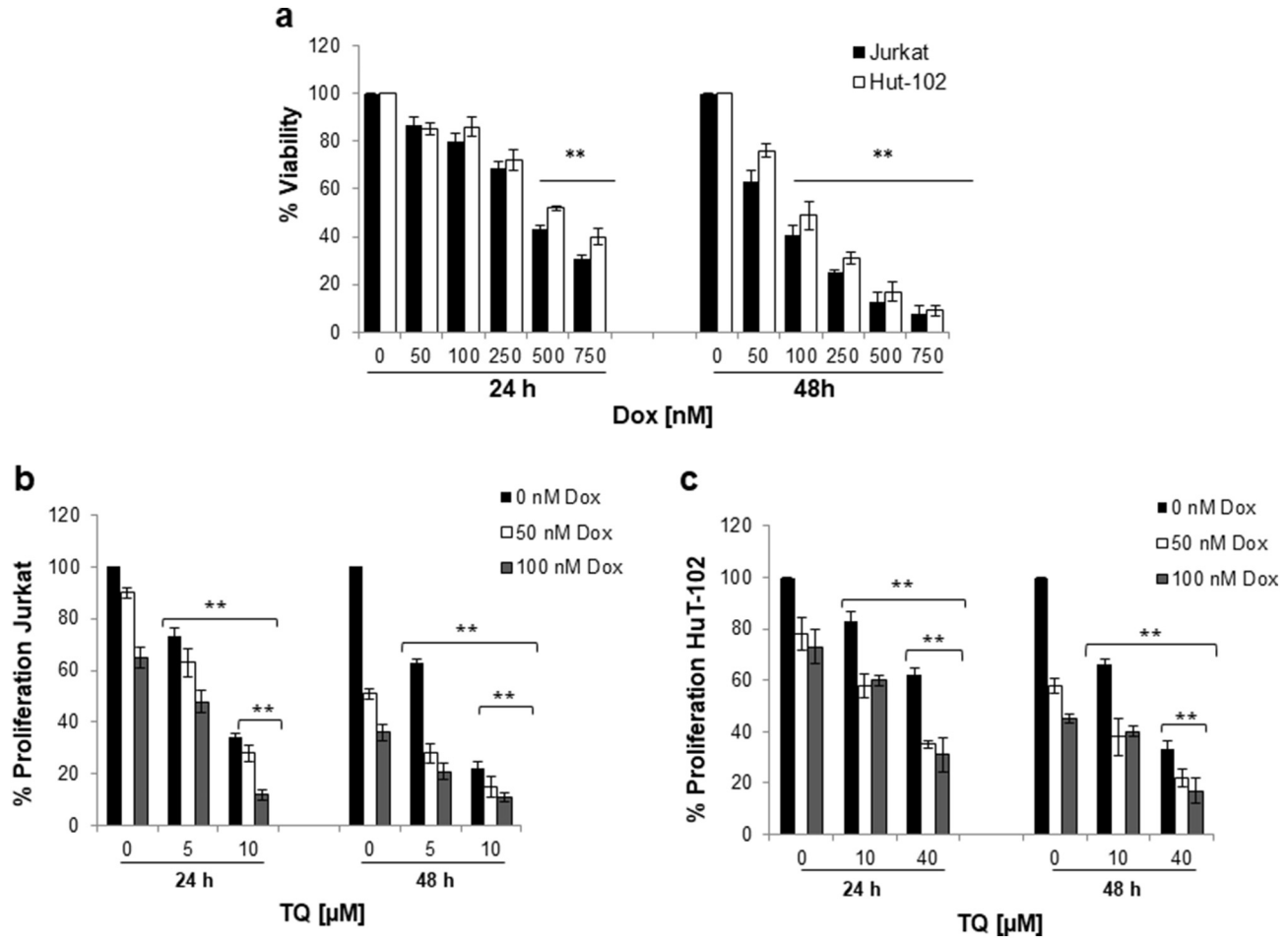

Fig. 1. The combination of TQ and Dox synergizes to reduce cell viability in Jurkat and HuT-102. a) HTLV-1 negative Jurkat cells and HTLV-1 positive HuT-102 cells were treated with Dox (50–750 nM). b) Jurkat cells and c) HuT-102 were treated with several combinations of TQ (0–10 μM) and Dox (0–100 μM). At 24 and 48 h post-treatment, cell viability was assessed by MTT assay and the values are expressed as % control. Each value represents the mean ± SD of three independent experiments. **($p < 0.01$) are significantly different from untreated control for each time point using two-tailed Student's *t*-test.

followed by flow cytometry. The data in Fig. 2 reveal that, compared to untreated controls or separate treatments, there was a noticeable time-dependent difference in cell cycle progression in both cell lines. The percentage of Jurkat cells in the Sub-G1 population increased from 6% to 28% upon treatment with 10 μM TQ at 24 h (Fig. 2a and Sup. Fig. 2). Similarly, the Sub-G1 population of HuT-102 cells at 48 h post-treatment with 40 μM TQ increased from 6% to 38% (Fig. 2b and Sup. Fig. 2).

As expected, treatment with Dox at 24 h significantly increased the G2/M cell population in both Jurkat and Hut-102 cells, suggesting G2/M arrest. Interestingly, treatment of both cell lines with TQ and Dox combinations synergized to significantly increase the percentage of cells in the Sub-G1 population in comparison to separate treatments.

3.3. TQ and Dox combination induces apoptosis via the mitochondrial pathway

We then confirmed if cell death triggered by the combination of TQ and Dox in both HTLV-1 positive and negative cell lines was due to apoptosis using TUNEL assay. As Fig. 3a demonstrates, treatment with Dox alone had insignificant apoptotic effects on both cell lines even after 48 h of exposure. The percentage of TUNEL positive cells did not exceed the 25% limit. On the other hand, treatment of Jurkat cells for 48 h with TQ (10 μM) or the combination led to 55% and 70% TUNEL positive cells, respectively. Similarly, treatment of HuT-102 cells for 48 h with TQ (40 μM) or the combination led to 65% and 90% TUNEL positive cells, respectively. The apoptotic effect of TQ alone was significant ($p < 0.05$) but when combined with Dox, this response was enhanced ($p < 0.01$). An early hallmark of apoptotic cell death is increased mitochondrial permeability, manifested by an increase in the mitochondrial membrane potential. To assess the integrity of the mitochondrial membrane, cells were treated with TQ, Dox or their combination. After treatment, staining with rhodamine 123 dye was performed and the mitochondrial membrane potential was measured as percentage of accumulated fluorescent dye. After 24 h, there was 31% and 56% of cells with disrupted mitochondrial membrane potential in Jurkat cells in response to TQ or the combination treatment, respectively (Fig. 3a). Similarly, treatment of HuT-102 cells for 48 h with TQ alone or the combination caused a major increase in the number of cells having decreased mitochondrial membrane potential (Fig. 3b). Similar to TUNEL results, TQ alone caused a significant disruption of the mitochondrial membrane potential, but the combination was more potent. In contrast, treatment of both cell lines with Dox alone did not appear to have a significant effect on the mitochondria.

3.4. The combination of TQ and Dox toxicity is associated with ROS generation, an effect reversed by pretreatment with the antioxidant NAC or pan caspase inhibitor

To investigate mechanisms involved in TQ and Dox cell death, we tested the involvement of ROS, since we have previously shown that TQ treatment caused apoptosis in Jurkat and HuT-102 cells by triggering

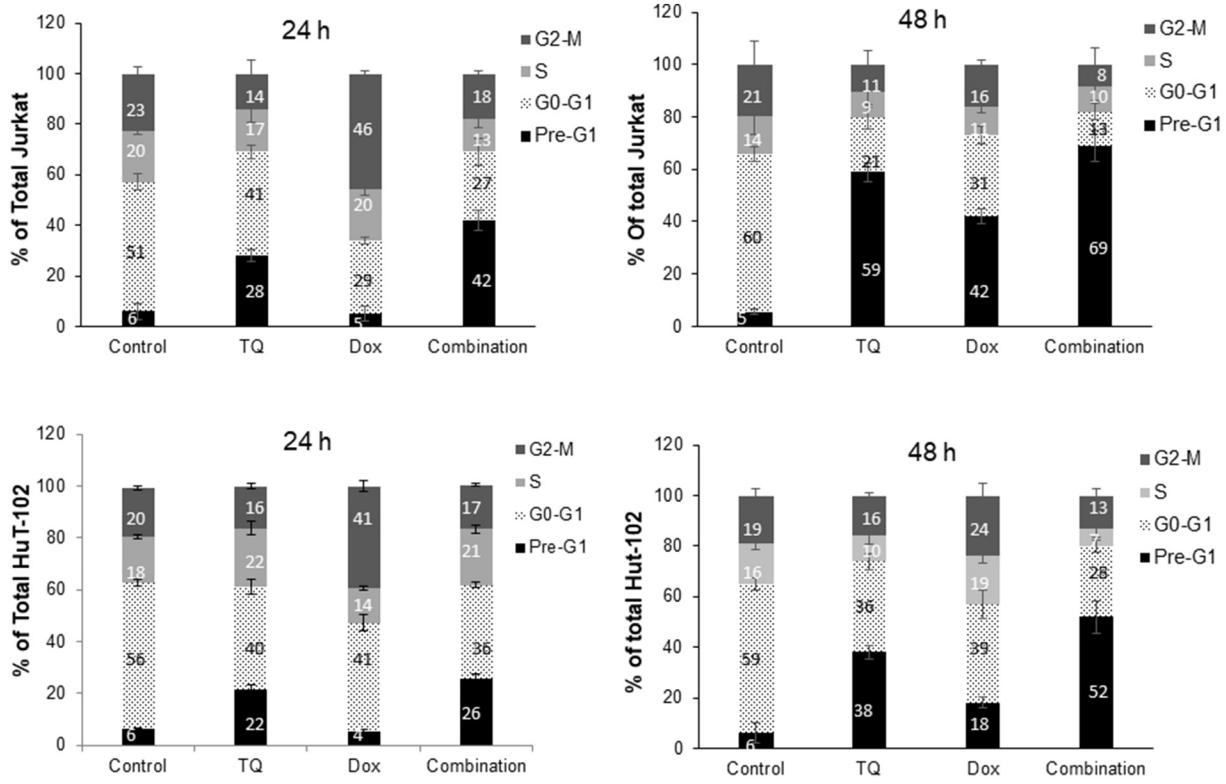

Fig. 2. The combination of TQ and Dox increases the sub-G1 population in Jurkat cells at 24 h and in HuT-102 cells at 48 h. a) Jurkat cells were treated with 10 μM TQ, 50 nM Dox or their combination. b) HuT-102 cells were treated with 40 μM TQ, 100 nM Dox or the corresponding combination for 24 or 48 h after which cells were stained with PI for flow cytometric analysis of DNA content with FACScan flow cytometry. The percentage of cells in the various stages of the cell cycle was calculated using Cell Quest. Each value is the mean ± SD of three independent experiments each done in duplicate.

the production of ROS [11]. To quantify ROS production, Jurkat and HuT-102 cells were treated with TQ, Dox or combinations for 1 h before treatment with the CM-H2DCFDA dye followed by flow cytometry analysis. Jurkat cells were treated with 10 μM TQ, 50 nM Dox or combinations and HuT-102 cells were treated with 40 μM TQ, 100 nM Dox or their combination. Quantification of ROS levels showed that both TQ and the combination treatment triggered ROS production in Jurkat cells while no significant ROS levels were noted upon treatment with Dox alone. As seen in Fig. 4a, both TQ and the combination treatment triggered around 40% increase in ROS production. In comparison, treatment with the positive control H2O2 triggered around 60% oxidative stress. Pretreatment of Jurkat cells with the strong antioxidant NAC was shown to completely abrogate ROS production by TQ and Dox combination. Similarly, ROS production increased in response to treatment of HuT-102 cells with TQ or the combination by around 30%.

To investigate whether caspases along with ROS participate in drug-induced apoptosis, we incubated the cells with either the general caspase inhibitor z-VAD-fmk (10 μM) or the antioxidant NAC (5 mM) for 2 h prior to treatment followed by viability assay, TUNEL assay and rhodamine staining. Pretreatment of cells with the antioxidant NAC or pan caspase inhibitor z-VAD-fmk partially protected both cell lines against combination treatment-induced cytotoxicity: in Jurkat cells, the viability increased from 26% to almost 65% whereas in HuT-102 cell viability increased from 27% to almost 60% at 48 h post-treatment (Sup. Fig. 3).

Western blotting of lysates of Jurkat and HuT-102 cells treated for 24 or 48 h was done to examine drug effects on the expression of proteins involved in apoptosis and multidrug resistance. As seen in Fig. 4b, treatment with TQ or the combination downregulated the expression of NFκB protein thus directing the cells towards apoptosis; an effect that was reversed upon pre-treatment with the antioxidant NAC. On the other hand, these treatments did not affect the expression levels of the oncogene p53 but increased its phosphorylation (phospho-p53) further carrying the cells towards programmed cell death. Neither Dox nor TQ treatment increased the expression of the multidrug resistance-associated protein (MRP1) in Jurkat or Hut-102 cells (Fig. 4b). Moreover, the combination treatment did not alter the expression of this protein.

Upon inhibiting caspases or scavenging ROS, the percentage of TUNEL positive cells at 48 h post-treatment decreased from 64% to 46% and 36% in Jurkat, and from 88% to 35% and 25% in HuT-102, respectively (Fig. 4c). A similar pattern was observed in the mitochondrial membrane potential assessment. In Jurkat, the population of cells with disrupted mitochondrial membrane potential decreased from 55% to 22% and 26% at 24 h posttreatment preceded with z-VAD-fmk and NAC pretreatment, respectively. On the other hand, the extent of reversal in the disruption of mitochondrial membrane potential upon z-VAD-fmk and NAC pretreatment was less pronounced in HuT-102 cells and ranged from 10 to 20% (Fig. 4d). These results suggest that apoptosis by TQ and Dox combination is ROS- and caspase-dependent.

3.5. TQ and Dox combination inhibit tumor volume in a xenograft ATL model more than single treatments

The ability of TQ and Dox combination to kill the aggressive HTLV-1 positive cells while avoiding the use of toxic doses of Dox is an attractive approach to study its *in vivo* antitumor potential and add some clinical relevance to our study. We developed an ATL xenograft model whereby HuT-102 cells (7.5 × 106) in Media:Matrigel (1:1 ratio) were subcutaneously inoculated into the right flank of NOD/SCID mice and showed efficient engraftment. Malignant palpable tumors were visualized within 7–9 days post-inoculation. To test the therapeutic efficacy of TQ and Dox combination in comparison to TQ or Dox alone, mice were divided into 4 groups of 6 mice each and injected intraperitoneally (i.p.) starting at day 9 post-inoculation with the

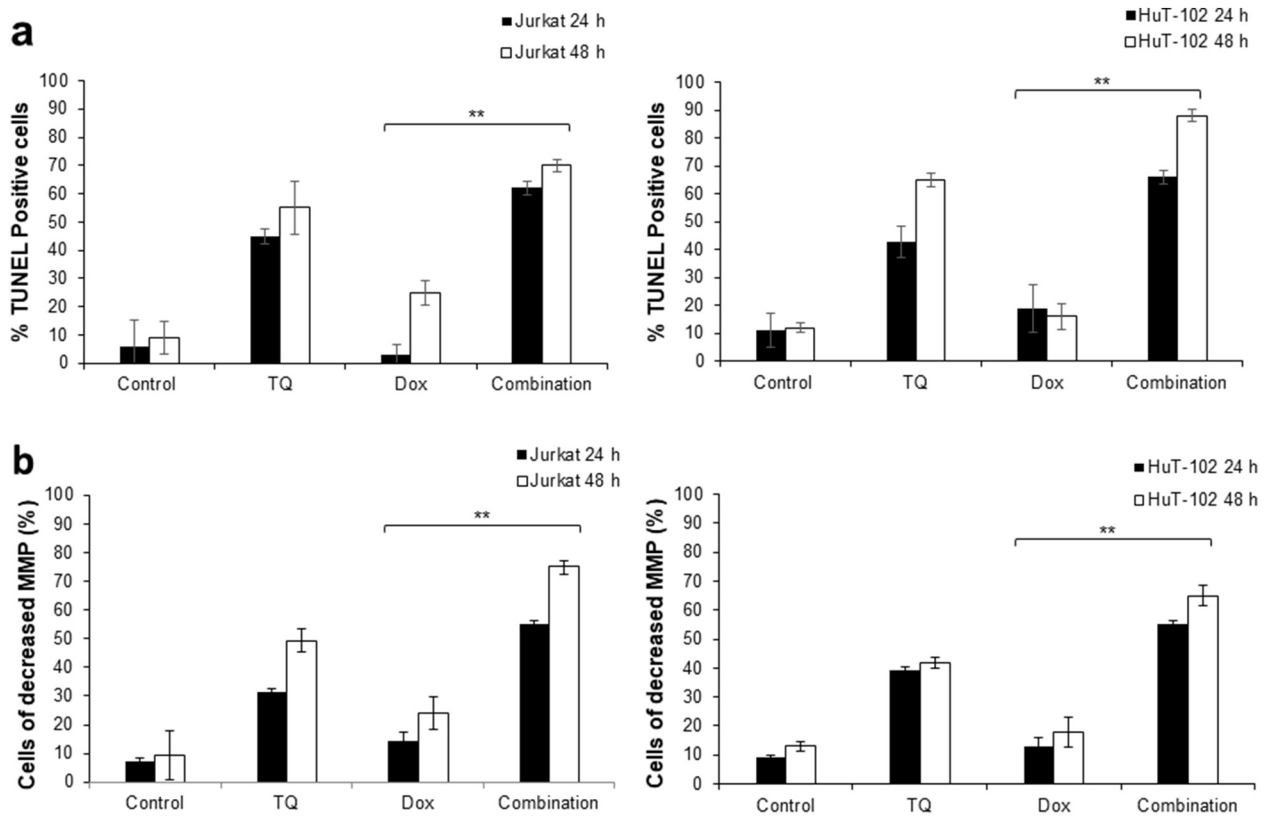

Fig. 3. The combination of TQ and Dox induces apoptosis *via* the mitochondrial pathway. Jurkat cells were treated with 10 μM TQ, 50 nM Dox or their combination. HuT-102 cells were treated with 40 μM TQ, 100 nM Dox or their combination for 24 h or 48 h. a) TUNEL assay measuring apoptotic cells in control and treated cells. b) Rhodamine assay measuring loss of mitochondrial membrane potential post-treatment. Each value is the mean ± SD of three independent experiments. TQ ($p < 0.05$) and combination ($p < 0.01$) were significantly different from the untreated control for each time point using two-tailed Student's *t*-test. **($p < 0.01$).

different treatments for 23 days. Tumor size and mice weight were monitored in all groups and measured every other day. As shown in Fig. 5a, Dox (0.5 mg/kg) alone had insignificant effects on tumor volume. The tumor remained relatively large and the final volume of the tumor was around 0.66 cm 3 compared to 1 cm^3 in the control group. On the other hand, TQ (20 mg/kg) injections decreased tumor volume by half compared to the control group (0.55 cm^3). Interestingly, combination treatment decreased the volume of tumors more significantly than either TQ or Dox alone starting from day 20. At the end of the experiment (day 28), the average volume of the tumors was around 0.3 cm^3. It is worth noting that TQ, Dox and combination were well tolerated as the mice weight did not decrease nor did they show signs of distress during the treatment period (Fig. 5b).

Histological H&E staining of tumor sections from the control mice showed malignant cell infiltration in the tissue. The high-grade tumor had irregular cell arrangements and intact tissue structure. A similar pattern was visualized in the tumors of the Dox treated group where the cells were highly dense with undamaged nuclei. In contrast, tumors from TQ and combination treated groups were considerably tightly packed in terms of structure. The tissue had decreased stroma with increased apoptotic dysregulated cells (impaired nuclei) suggesting tumor destruction, a result consistent with the tumor growth profile (Fig. 5c). Consistently, the expression of the nuclear proliferation marker Ki-67 was the highest in the control group followed by the Dox treated group. However, in TQ and combination treated groups, the expression of Ki-67 was significantly lower as depicted by immunostaining. Furthermore, *in vivo* TQ and TQ and Dox combination induced apoptosis in the tumor tissues as conveyed by TUNEL staining. Collectively, these data confirm that combining TQ with low doses of Dox is effective in inhibiting ATL xenografts compared to Dox alone, a tactic that could hijack Dox undesirable toxic effects (Fig. 5c and d).

4. Discussion

Adult T-cell leukemia is an aggressive liquid malignancy caused by HTLV-1 viral infection [1]. Due to intrinsic chemo-resistance and immunosuppression, ATL patients have poor prognosis. Despite the current progress in ATL therapeutics, the treatment options are extremely limited, and there are no clear treatment recipes that work well in the long term including the orthodox antineoplastic agents used in the clinic [20]. In addition, the use of higher doses of drugs in ATL patients has not significantly improved the overall survival rate but instead has caused resistance and undesirable toxic effects [21].

In an attempt to find a safe and an effective treatment option, we investigated the use of TQ, a plant derived compound, in combination with Dox, a commonly used chemotherapeutic agent for the treatment of advanced solid tumors and acute leukemia [22]. The central finding of the present investigation is that low doses of Dox in combination with TQ significantly inhibit the viability of HTLV-1 negative and HTLV-1 positive cells and enhance their cell death, in a caspase- and ROS-dependent manner, in comparison to treatment with Dox alone. The significance of this finding is attributed to the fact that Dox is a well-known cancer therapeutic agent but causes harmful effects on patients' health. The latter include cardiomyopathy, immunosuppression and the development of primary and secondary drug resistance in tumor cells, all of which limit Dox clinical success in cancer chemotherapy [23].

Overall, we observed that the anticancer effects of Dox are achieved at half its concentration or even less when combined with 10 μM (Jurkat) or 40 μM of TQ (HuT-102). The results of our study show an increased therapeutic effect of Dox in combination with TQ and strongly support our hypothesis that combination of natural compounds like TQ, along with reducing the dosage of a conventional

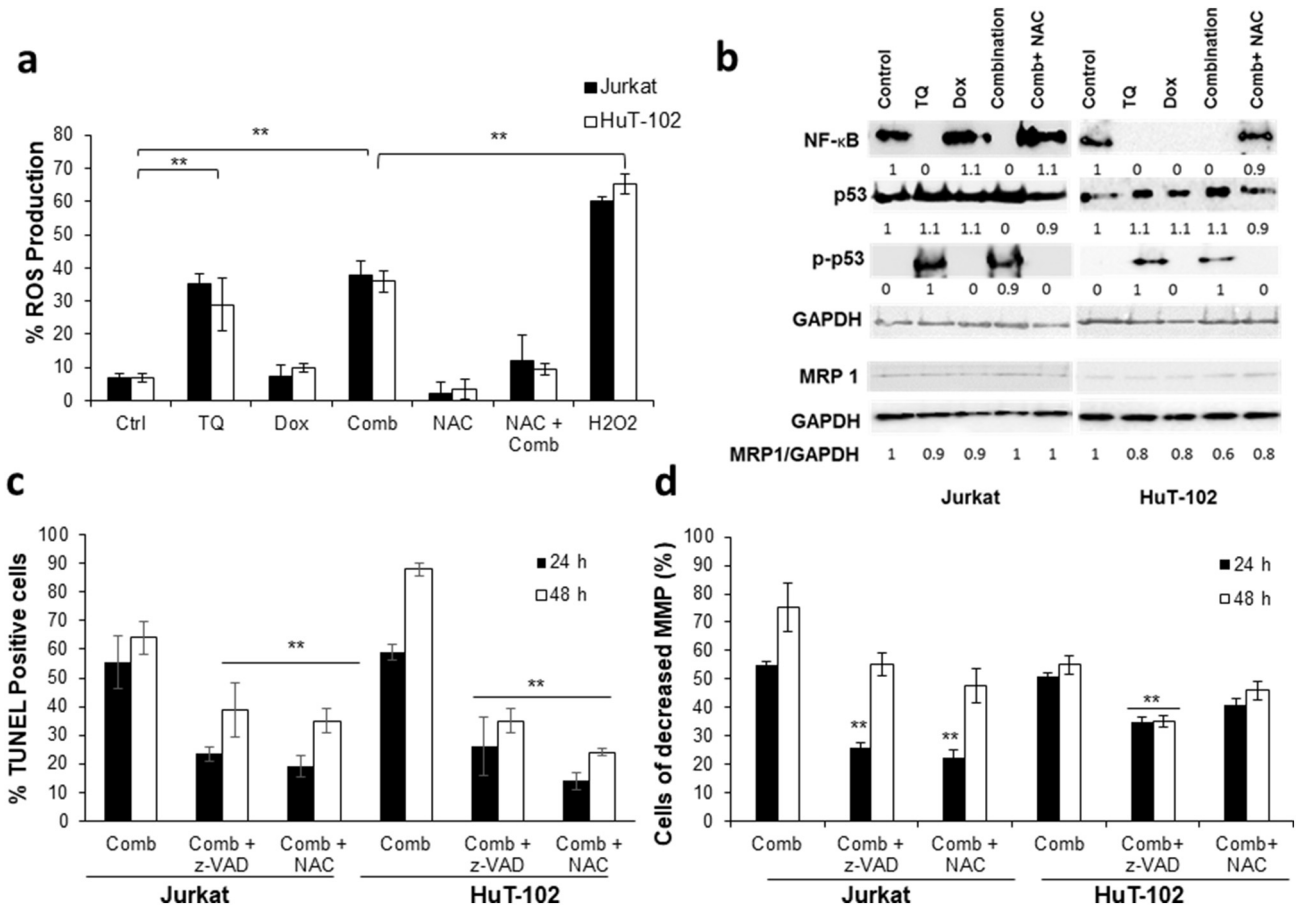

Fig. 4. Pretreatment with NAC and z-VAD-fmk protect malignant T-cells against TQ and Dox induced ROS generation and toxicity. a) Jurkat cells were treated with 10 μM CM-H2DCFDA dye for 20 min, and then treated for 1 h with 10 μM TQ, 50 nM Dox, the combination treatment (with or without pre-treatment with NAC) or with H_2O_2 (150 μM). HuT-102 cells were treated with 10 μM CMH2DCFDA dye for 20 min, and then with 40 μM TQ, 100 nM Dox, their combination (referred to as Comb) or H_2O_2 (150 μM) for 1 h. After treatment, the cells were collected and analyzed by flow cytometry. b) Jurkat cells were treated with 10 μM TQ, 50 nM Dox or their combination for 24 h. HuT-102 cells were treated with 40 μM TQ, 100 nM Dox or their combination for 48 h. After treatment, the cells were lysed and proteins were extracted for analysis. Western blot analysis was conducted with the corresponding primary antibodies to study the expression of p53, p-p53 and NF-kB. GAPDH was used as a reference loading control. c) TUNEL assay and d) Rhodamine assay in cells pretreated with the antioxidant NAC (5 mM) or z-VAD-fmk pan caspases inhibitor (10 μM). Each value in plots a, c and d are the mean ± SD of three independent experiments. *($p < 0.05$) and **($p < 0.01$) are significantly different from untreated control for each time point using two-tailed Student's *t*-test.

chemotherapeutic agent, may retain the benefits of minimizing the undesirable toxicity against normal cells. Higher concentrations and longer incubation times of Dox and TQ combination were required to reduce the viability of the resistant HuT-102 cells. The differences in treatment responses of the two cell lines could be attributed to their genomic differences including the expression of the viral oncoprotein Tax whose role in conferring resistance to apoptosis for HTLV-1 positive cells is well established [4,24].

Unlike treatment with Dox which caused G2/M arrest, treatment with TQ or the combination mediated cell death by apoptosis in both cell lines. This is consistent with literature showing that Dox induces G2/M arrest in leukemia cells [25]. TQ and the combination treatment but not Dox were able to induce ROS production. Most cancer cells have high ROS levels which promote and maintain their high cell proliferation level [26]. An increase in the ROS levels beyond a threshold, however, can result in growth arrest, senescence or even cell death by apoptosis. Both TQ and Dox cytotoxic effects are known to be partially mediated by pro-oxidation [9,27]. However, in the described combination treatments, Dox used at low concentrations did not trigger ROS production. This could be due to the fact that, in both cell lines, Dox was applied at concentrations below the IC_{50} value. TQ's ability to interact with glutathione and other thiol-bearing enzymes, and deplete the intracellular thiols could thus account for the oxidative stress induced after treatment with TQ or the combination.

In addition to ROS production, the combination treatment was able to disturb the mitochondrial membrane potential of both cell lines, an early sign of intrinsic apoptosis or apoptosis through the mitochondrial route. The increase in the mitochondrial membrane potential after using an inhibitor of caspases confirms the association between cell death through caspases activation and the mitochondria, and suggest that the drug combination could be mediating cell death by apoptosis through the intrinsic pathway. Western blot analysis further confirmed the implication of the apoptotic pathway in response to the treatment with the combination. Interestingly, TQ and the combination inhibited the transcription factor NF-κB expression and triggered the stabilization of p53 through its phosphorylation, thereby directing the cells towards apoptosis. Similarly, treatment with Dox alone abrogated the expression of the proliferation marker NFκB, probably due to its ability to induce cell cycle arrest at G2/M. This finding is in accordance with the observed Dox effects on NF-κB expression in MCF-7 breast cancer cells [28] and HT-28 colon cancer cells [29]. In our cell system, it appears that the MRP1 protein is not involved in the effects of either drug or the combination treatment.

In vivo, when combined with Dox, TQ suppressed tumor growth in the ATL xenograft mouse model more significantly than separate treatments. The mechanism of inhibition of tumor volume by

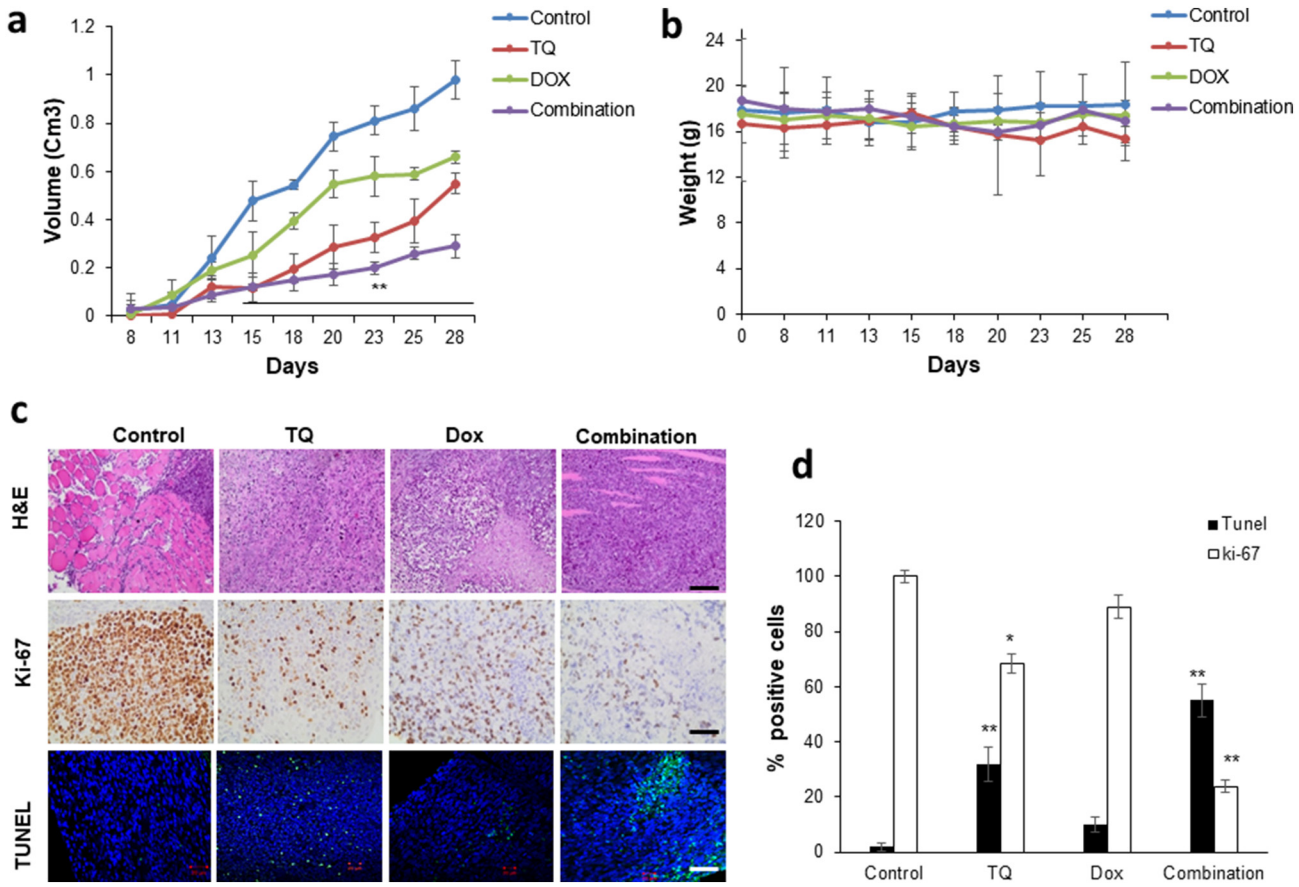

Fig. 5. The combination of TQ and Dox decreases the volume of ATL cancer xenografts in mice. Graphs showing a) the tumor volume and b) weight of mice given HuT-102 xenografts and injected with 20 mg/kg TQ i.p., three times per week for 24 days, 0.5 mg/kg Dox i.p. one time per week for 23 days. Tumor volumes were significantly smaller in combination-treated mice as compared to lipfundin® injected (Ctrl) starting at day 11 after treatment (mean ± SD, n = 6 mice per group, ** $p < 0.01$, significant difference with respect to Control). c) Histological (H & E) and immunohistochemical (Ki-67 antibody) staining in tumor xenografts. Apoptosis staining is revealed by using the TUNEL assay. Tissue was processed as described in "Methods." Identical fields are shown for fluorescein-labeled detection of TUNEL-positive nuclei (green fluorescence). Representative images were taken at 400× magnification. Scale bar = 50 µm. d) Percentage of TUNEL positive and Ki-67 positive cells with respect to the total number of counted cells. Images were processed using Image J. The bar graph represents data (mean ± SD) from four different stained slides each with > 500 cells. *($p < 0.05$) and **($p < 0.01$) are significantly different from untreated control using two-tailed Student's *t*-test. (For interpretation of the references to color in this figure legend, the reader is referred to the web version of this article.)

combination of TQ and Dox was mainly through the inhibition of proliferation in tumors and increased apoptotic response as evidenced by the decrease in Ki67 expression and increase in TUNEL positive cells in tumor sections. Extensive evidence from animal studies shows that TQ improves the therapeutic efficacy of many chemotherapeutic agents including Dox by enhancing their antitumor activity and/or decreasing their toxicity to normal cells [21,30,31]. Interestingly, our findings confirm the synergy between TQ and Dox that could be attributed to TQ's adjuvant potential and ability to augment the therapeutic effects of Dox.

5. Conclusion

To sum up, the combination of TQ with the anthracyclin Dox offers the possibility to use up to twofold lower doses of Dox while exhibiting the same cancer inhibitory effect against ATL both *in vitro* and *in vivo*. Although cell death is higher upon treatment with TQ and Dox combination as compared to separate drugs, most of the mechanisms implicated in response to combination treatment, namely apoptosis, disruption of the mitochondrial membrane potential, ROS, and regulation of the expression of key molecular targets, seem to be similar to those observed upon treatment with TQ alone. The effect of treatment with the twofold higher doses of Dox on these mechanisms is the subject of future studies in order to better understand the implications of using higher doses of Dox in combination with TQ.

Supplementary data to this article can be found online at https://doi.org/10.1016/j.lfs.2019.116628.

Acknowledgments

This work was supported by the Lebanese National Council for Scientific Research (LNCSR) (Project number: 24314, Award: 103482/103487). We thank Dr. Assaad Eid (Professor, Department of Anatomy, Cell Biology and Physiological Sciences, AUB) for providing the MRP1 antibody. We would also like to thank members of the Kamal Shair Central Research Science Laboratory for helping with flow cytometry analysis and microscopy imaging.

Declaration of Competing Interest

The authors declare that they have no competing interests.

References

[1] C.Z. Giam, O.J. Semmes, HTLV-1 infection and adult t-cell leukemia/lymphoma-a tale of two proteins: tax and HBZ, Viruses 8 (6) (2016) 16. pii: E161.
[2] M. Matsuoka, K.T. Jeang, Human T-cell leukaemia virus type 1 (HTLV-1) infectivity and cellular transformation, Nat. Rev. Cancer 7 (2007) 270–280.
[3] M.D. Lairmore, R. Haines, R. Anupam, Mechanisms of human T-lymphotropic virus

type 1 transmission and disease, Curr Opin Virol 2 (2012) 474–481.
[4] R.C. Gallo, L. Willems, Y. Tagaya, Time to go back to the original name, Front. Microbiol. 8 (2017) 1800.
[5] I. Azran, Y. Schavinsky-Khrapunsky, M. Aboud, Role of tax protein in human T-cell leukemia virus type-I leukemogenicity, Retrovirology 1 (2004) 20.
[6] M. Boxus, J.C. Twizere, S. Legros, J.F. Dewulf, R. Kettmann, L. Willems, The HTLV-1 tax interactome, Retrovirology 5 (2008) 76.
[7] S. Fochi, S. Mutascio, U. Bertazzoni, D. Zipeto, M.G. Romanelli, HTLV deregulation of the NF-kappaB pathway: an update on tax and antisense proteins role, Front. Microbiol. 9 (2018) 285.
[8] C.C. Woo, A.P. Kumar, G. Sethi, K.H. Tan, Thymoquinone: potential cure for inflammatory disorders and cancer, Biochem. Pharmacol. 83 (2012) 443–451.
[9] R. Schneider-Stock, I.H. Fakhoury, A.M. Zaki, C.O. El-Baba, H.U. Gali-Muhtasib, Thymoquinone: fifty years of success in the battle against cancer models, Drug Discov. Today 19 (2014) 18–30.
[10] H. Gali-Muhtasib, A. Roessner, R. Schneider-Stock, Thymoquinone: a promising anti-cancer drug from natural sources, Int. J. Biochem. Cell Biol. 38 (2006) 1249–1253.
[11] E.M. Dergarabetian, K.I. Ghattass, S.B. El-Sitt, R.M. Al-Mismar, C.O. El-Baba, W.S. Itani, N.M. Melhem, H.A. El-Hajj, A.A. Bazarbachi, R. Schneider-Stock, H.U. Gali-Muhtasib, Thymoquinone induces apoptosis in malignant T-cells via generation of ROS, Front Biosci (Elite Ed) 5 (2013) 706–719.
[12] Y. Octavia, C.G. Tocchetti, K.L. Gabrielson, S. Janssens, H.J. Crijns, A.L. Moens, Doxorubicin-induced cardiomyopathy: from molecular mechanisms to therapeutic strategies, J. Mol. Cell. Cardiol. 52 (2012) 1213–1225.
[13] R. Bayat Mokhtari, T.S. Homayouni, N. Baluch, E. Morgatskaya, S. Kumar, B. Das, H. Yeger, Combination therapy in combating cancer, Oncotarget 8 (2017) 38022–38043.
[14] S.N. Goyal, C.P. Prajapati, P.R. Gore, C.R. Patil, U.B. Mahajan, C. Sharma, S.P. Talla, S.K. Ojha, Therapeutic potential and pharmaceutical development of thymoquinone: a multitargeted molecule of natural origin, Front. Pharmacol. 8 (2017) 656.
[15] K. Effenberger-Neidnicht, R. Schobert, Combinatorial effects of thymoquinone on the anti-cancer activity of doxorubicin, Cancer Chemother. Pharmacol. 67 (2011) 867–874.
[16] S.A. Arafa el, Q. Zhu, Z.I. Shah, G. Wani, B.M. Barakat, I. Racoma, M.A. El-Mahdy, A.A. Wani, Thymoquinone up-regulates PTEN expression and induces apoptosis in doxorubicin-resistant human breast cancer cells, Mutat. Res. 706 (2011) 28–35.
[17] O.A. Al-Shabanah, O.A. Badary, M.N. Nagi, N.M. al-Gharably, A.C. al-Rikabi, A.M. al-Bekairi, Thymoquinone protects against doxorubicin-induced cardiotoxicity without compromising its antitumor activity, J. Exp. Clin. Cancer Res. 17 (1998) 193–198.
[18] O.A. Badary, A.B. Abdel-Naim, M.H. Abdel-Wahab, F.M. Hamada, The influence of thymoquinone on doxorubicin-induced hyperlipidemic nephropathy in rats, Toxicology 143 (2000) 219–226.
[19] M.N. Nagi, M.A. Mansour, Protective effect of thymoquinone against doxorubicin-induced cardiotoxicity in rats: a possible mechanism of protection, Pharmacol. Res. 41 (2000) 283–289.
[20] A. Marcais, F. Suarez, D. Sibon, L. Frenzel, O. Hermine, A. Bazarbachi, Therapeutic options for adult T-cell leukemia/lymphoma, Curr. Oncol. Rep. 15 (2013) 457–464.
[21] O. Hermine, J.C. Ramos, K. Tobinai, A review of new findings in adult t-cell leukemia-lymphoma: a focus on current and emerging treatment strategies, Adv. Ther. 35 (2018) 135–152.
[22] F. Yang, S.S. Teves, C.J. Kemp, S. Henikoff, Doxorubicin, DNA torsion, and chromatin dynamics, Biochim. Biophys. Acta 1845 (2014) 84–89.
[23] Y. Chen, Y. Wan, Y. Wang, H. Zhang, Z. Jiao, Anticancer efficacy enhancement and attenuation of side effects of doxorubicin with titanium dioxide nanoparticles, Int. J. Nanomedicine 6 (2011) 2321–2326.
[24] A. Muhleisen, M. Giaisi, R. Kohler, P.H. Krammer, M. Li-Weber, Tax contributes apoptosis resistance to HTLV-1-infected T cells via suppression of Bid and Bim expression, Cell Death Dis. 5 (2014) e1575.
[25] R. Nowak, J. Tarasiuk, Retaining cytotoxic activity of anthrapyridone CO1 against multidrug resistant cells is related to the ability to induce concomitantly apoptosis and lysosomal death of leukaemia HL60/VINC and HL60/DOX cells, J. Pharm. Pharmacol. 65 (2013) 855–867.
[26] G.Y. Liou, P. Storz, Reactive oxygen species in cancer, Free Radic. Res. 44 (2010) 479–496.
[27] P. Angsutararux, S. Luanpitpong, S. Issaragrisil, Chemotherapy-induced cardiotoxicity: overview of the roles of oxidative stress, Oxidative Med. Cell. Longev. 2015 (2015) 795602.
[28] F. Ashour, M.H. Awwad, H.E. Sharawy, M. Kamal, Estrogen receptor positive breast tumors resist chemotherapy by the overexpression of P53 in cancer stem cells, J Egypt Natl Canc Inst 30 (2) (2018) 45–48.
[29] C. Riganti, S. Doublier, C. Costamagna, E. Aldieri, G. Pescarmona, D. Ghigo, A. Bosia, Activation of nuclear factor-κB pathway by simvastatin and RhoA silencing increases doxorubicin cytotoxicity in human colon cancer HT29 cells, Mol. Pharmacol. 74 (2) (2008) 476–484.
[30] N.E. El-Ashmawy, E.G. Khedr, E.M. Ebeid, M.L. Salem, A.A. Zidan, E.M. Mosalam, Enhanced anticancer effect and reduced toxicity of doxorubicin in combination with thymoquinone released from poly-N-acetyl glucosamine nanomatrix in mice bearing solid Ehrlish carcinoma, Eur J Pham Sci 109 (2017) 525–532.
[31] N.M. Elsherbiny, M. El-Sherbiny, Thymoquinone attenuates doxorubicin-induced nephrotoxicity in rats: role of Nrf2 and NOX4, Chem. Biol. Interact. 223 (2014) 102–108.